



Subretinal injections in rodent eyes: Effects on electrophysiology and histology of rat retina

Adrian M. Timmers, Hong Zhang, Alicia Squitieri, Carlos Gonzalez-Pola

Department of Ophthalmology, University of Florida, Gainesville, FL

Purpose: To describe a reliable and fast method for subretinal injection in rodents and to assess the effect of the procedure on retinal function and histology.

Methods: Corneas of rodents were punctured with a 28 gauge hypodermic insulin needle avoiding the lens. The injection procedure can be observed with the aid of a dissecting microscope and methylcellulose solution on the eye. A 33 gauge blunt needle was inserted into the eye through the corneal puncture and guided toward the subretinal matrix. Addition of fluorescein to the injection mixture facilitated immediate evaluation of the injection. Rat eyes were either non-injected (controls), received only a corneal puncture or were injected with fluorescent microspheres or PBS-fluorescein mixture. Retinal function and integrity were assessed through electroretinographic (ERG) analysis and postmortem histology.

Results: The anterior injection procedure provided a fast and simple method for subretinal injections. In rats a successful subretinal delivery was achieved in more than 90%, with less than 5% of the injected eyes developing cataracts. No significant differences in b-wave ERG amplitudes in rodent eyes over a five-week period were observed between non-injected control eyes and subretinally injected eyes (1 to 10 μ l of PBS-fluorescein or 2 μ l fluorescent microspheres). Histological analysis revealed that re-attachment of the rat retina occurred in approximately 1 day post-injection and the phagocytotic ability of RPE cells remained intact.

Conclusions: This method was easily learned and required a minimum of equipment and animal preparation. With experience, 10 to 30 eyes could be injected per h. Furthermore, the injection procedure did not compromise the lens, retina or retinal pigment epithelium (RPE).

For development of gene therapy strategies of degenerative diseases of the retina, pioneering experiments are performed on the eyes of rats and mice carrying spontaneous or engineered mutations. A variety of studies of viral transgene delivery to rodent ocular tissue have been published ranging from survival factor expression to gene augmentation and down regulation of genes [1-24]. All these studies required intraocular injections, either subretinal or vitreal. Surprisingly, the injection methods applied are not described in great detail and documentation describing the effects of such injections on the integrity of the retina is completely absent.

Our studies on viral transgene delivery for rescue or degenerative goals require a dependable, simple and expedient method for subretinal injections in rats and mice. A method that meets these standards is a procedure first alluded to by Cepko and co-workers [25,26]; the effects on retinal function have not been described. However, there is some evidence that subretinal injections affect photoreceptor cells. For instance, subretinal "dry-needle" sham injections temporarily protected photoreceptor cells proximal to the injection site from light damage or degeneration in the RCS rats [27,28]. Therefore, our objective was to systematically characterize the effects of the injection method on retinal function and histology.

In this paper, we describe in detail an adaptation of the injection procedure exiguously described in 1987 [25,26]. Rat eyes were injected subretinally and the integrity of the retina was assessed by weekly ERG measurements for five weeks followed by histological analysis of the retina. The electrophysiology and histology of retinas in eyes that received subretinal injections of phosphate buffered saline were similar to non-injected eyes.

METHODS

Animals: Sprague Dawley male rats of approximately 200 g were purchased from Harlan and maintained under 12 h light:12 h dark cyclic lighting conditions. All animals were treated according to ARVO Statements for the Use of Animals in Ophthalmic and Vision Research, guidelines comparable to Public Health Service Policy on Humane Care and Use of Laboratory Animals (US Public Health Service).

Anesthesia and mydriasis: Rats were anesthetized by intraperitoneal injection with a mixture of 12.5 mg/kg xylazine (Butler Company, Columbus, OH) and 62.5 mg/kg ketamine (Phoenix Pharmaceutical, St. Joseph, MO). Pupils were dilated with 2.5% phenylephrine (Akorn, Inc., Decatur, IL), and 0.5% proparacaine (Alcon Laboratories Inc., Fort Worth, TX) was applied for topical anesthesia. The vibrissae were trimmed to get an unobstructed view of the eye and fundus. The time needed to achieve a deep plane of anesthesia sufficed to complete pupil dilation. Degree and progression of mydriasis was checked with a SMZ-1 dissecting microscope (Nikon, Melville,

Correspondence to: Adrian M. Timmers, Ph.D., Department of Ophthalmology, Box 100284 JHMHC, Room D4-38D, University of Florida, Gainesville, FL, 32610-0284; Phone: (352) 392-0747; FAX: (352) 392-0573; email: atimmers@eye1.eye.ufl.edu

NY). A second application of mydriatic and topical anesthetic drops was used as the anesthetics began to take effect. The deep anesthetic plane was maintained for 20 to 30 min, providing ample time to perform subretinal injections, fundus photography or ERG. Immediately following the injection procedure an ophthalmic ointment containing bacitracin, neomycin and polymyxins was applied to prevent corneal opacification and to reduce risks of infection.

Subretinal injections: Following complete dilation, the anesthetized animal was placed in lateral recumbency under the SMZ-1 Nikon dissecting microscope and positioned with one holding hand. The rat fundus could be visualized with the

application of a drop of 2.5% methylcellulose to the eye. The cornea was carefully punctured nasally approximately 0.5 to 1 mm medial to the dilated pupillary margin with a 28 gauge hypodermic needle (Becton Dickinson & Company, Franklin Lakes, NJ). The needle with bevel up was advanced full thickness through the cornea into the anterior chamber parallel to the anterior lens face. At least 50% of the bevel was pushed through the cornea to produce a hole sufficiently large to insert the 33 gauge blunt needle (Hamilton Company, Reno, NV). The blunt needle tip was inserted through the corneal puncture and advanced into the anterior chamber, avoiding trauma to the iris and lens. Subsequently, the needle shaft was aimed

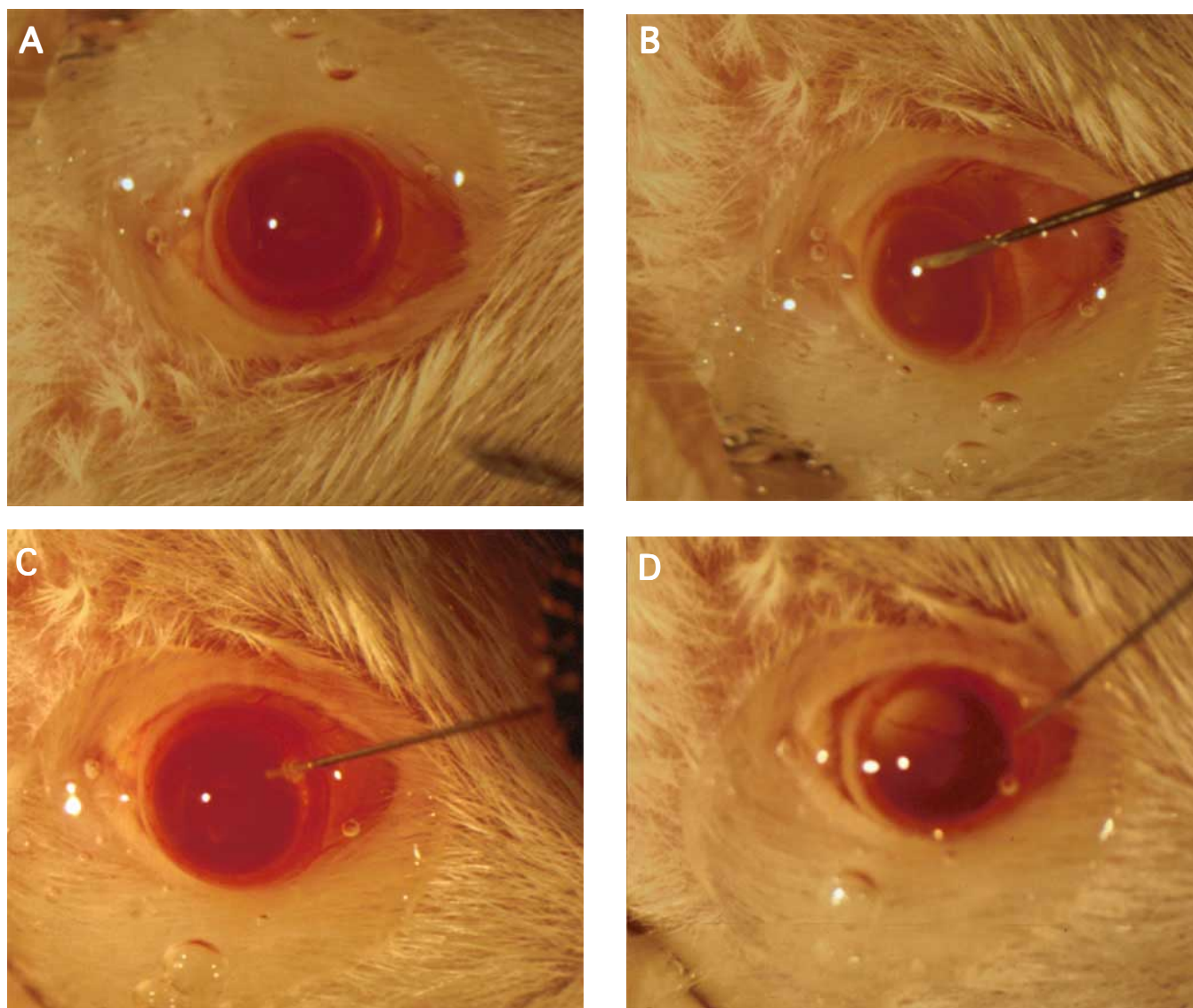


Figure 1. Subretinal injections in rodent with anterior approach. Series of images of Sprague Dawley rat eyes during the injection procedure. The rats were anesthetized with a mixture of ketamine and xylazine; phenylephrine and a topical anesthetic were applied to the eyes. **A:** Complete mydriasis prior to injection. **B:** Corneal puncture of the eye with a 28 gauge needle. Approximately 70 to 100% of the bevel has been advanced into the anterior chamber, the point of puncture was approximately 1.5 mm medial to the pupillary margin. **C:** The 33 gauge blunt needle tip in the anterior chamber of the punctured eye. Subsequently, the needle was angled to point slightly nasally and guided posteriorly into the eye toward the injection site. Upon penetration of the retina, a PBS-fluorescein mixture was deposited subretinally. **D:** After injection of 2 μ l of PBS-fluorescein mixture, the retinal bleb is visible with the dye located subretinally. Note the retinal blood vessel overlying the green bleb indicative of a successful subretinal injection.

slightly nasally toward the posterior chamber with the iris lateral and lens medial. The lens was displaced medially as the needle was advanced toward the desired injection location. A slight resistance to the movement of the needle indicated penetration of the retina and entrance into the subretinal matrix. At this time the syringe was held in place and an assistant pushed the plunger slowly in approximately 30 s injecting the contents of the syringe into the subretinal matrix creating a visible retinal detachment. Following subretinal delivery, the needle was gently withdrawn. We routinely administered a small amount of fluorescein (0.1 mg/ml final concentration) with the injection material to visualize the injection and bleb formation. Occasionally a small amount of injected material would reflux through the corneal wound, this could be avoided by releasing any holding pressure onto the rat during the injection procedure.

Fundus photography: The animals were anesthetized and pupils were dilated as described above. The rat fundus was viewed with a Genesis Kowa handheld fundus camera in conjunction with a Super 66 Volk Stereo Fundus lens mounted between camera and eye. The setup for fundus photography was adapted from Hawes et al. [29]. For regular fundus photography, Kodak 100 Ektachrome film and for fluorescence fundus photography Kodak P1600 Ektachrome film was used.

ERG analysis: Following overnight dark adaptation, the animals were anesthetized and the pupils were dilated. All procedures were carried out under dim red light (>650 nm). ERGs from both eyes were recorded simultaneously using the UTAS-E 2000 Visual Electrodiagnostic System (LKC Technologies, Gaithersburg, MD). Gold contact lens electrodes were placed on the eyes with a drop of methylcellulose [30]. A reference electrode was placed subcutaneous on the head and a ground electrode in the right hind leg. The animals were



Figure 2. Subretinal injection with PBS-fluorescein mixture.. Rat eye subretinally injected with 2 μ l of PBS-fluorescein mixture. Note the retinal blood vessel overlying the green bleb. In case of a vitreal injection, the retinal vessels would be obscured by the fluorescein which could fill the entire eye.

placed in a Ganzfeld illumination dome. Full field scotopic ERGs of both eyes were elicited simultaneously with 10 μ s flashes of blue light. Electrical responses detected at the corneal contact electrodes were amplified at a gain setting of 4000 and filtered between 0.3 and 3000 Hz. Digitations were done on both channels at a rate of 2 KHz. Routinely 5 recordings per flash intensity were averaged. The intervals between flashes increased from 10 s to 30 s with increasing flash intensity. Recordings were standardly obtained at four increasing intensities of blue light (-5.1 to -1.84 log cd*s*m⁻²). ERGs were evaluated based on b-wave amplitude (the voltage difference between a-wave and b-wave). The b-wave amplitudes for each flash intensity were determined. For each eye, the b-wave amplitudes obtained before the injection were set at 100%, the amplitudes determined for the subsequent weeks were then calculated relative to the pre-injection amplitudes.

Tissue preparation and sections: Asphyxiation of the animal under carbon dioxide was immediately followed by cervical dislocation. The thoracic cavity was entered to expose the heart and the descending thoracic aorta was identified and occluded with hemostatic forceps. The apex of the heart was transected to access the left ventricular lumen. A blunted 19 gauge needle sheathed with silastic tubing was advanced through the left ventricle into the proximal ascending aorta and clamped in place at the ventricular opening with hemostats. The right atrium was cut to allow efflux of blood and perfusate. Placing the containers with perfusion solutions approximately 1.3 m higher than the animal provided the appropriate pressure for the perfusion. First, the animal was perfused with phosphate buffered saline, pH 7.4 (PBS) for approximately 3 min (until the efflux was clear) followed by freshly prepared 4% paraformaldehyde in PBS. Approximately 150 ml of fixation solution per rat provided complete fixation of ocular tissues. Prior to enucleation, the eye was marked superiorly with a suture or branded with a heated 28 gauge needle. Following enucleation, the cornea was punctured and the eye was fixed for an additional 2 h at 4 °C in 4% paraformaldehyde in PBS. Subsequently the cornea, lens and vitreous were removed without disturbing the retina. The eyecup was sunk in 30% sucrose in PBS for at least 1 h, routinely overnight at 4 °C. The eyecup was embedded in Tissue-Tek O. C. T. 4583 cryostat compound (Sakura Finetek USA, Inc., Torrance, CA) and frozen in a bath of CO₂-ethanol. Serial sections (15 μ m) were cut on a HM 505 E Cryostat (Micron, Walldorf, Germany). Non-stained sections were viewed on an Axioplan 2 Fluorescence microscope (Carl Zeiss Inc., Thornwood, NY) using fluorescein filter settings to visualize the fluorescent microspheres; digital images were obtained with a SPOT digital camera (Diagnostic Instrument, Inc., Sterling Heights, MI).

RESULTS & DISCUSSION

Injection procedure: Various surgical complications to ocular tissues can result from subretinal injections using the anterior approach. These complications include trauma to cornea, iris, retina and most importantly lens. Our initial attempts to inject subretinally following the procedure described by Cepko

and co-workers [25,26] resulted in frequent cataract formation (25 to 40%). These cataracts resulted from damage inflicted on the lens as the cornea was punctured and/or as the blunt needle was directed toward the subretinal matrix. The following modifications reduced the incidence of cataract formation. The cornea was punctured with a 28 gauge needle with its bevel up (Figure 1). Upon full thickness penetration of the cornea, slight traction allowed advancement of the needle without laceration of the anterior capsule and cortical lens. In order to minimize damage and provide adequate entry for insertion of the 33 gauge blunt needle, advancement of approximately 50% of the bevel through the cornea was needed. Upon withdrawal, again injury to the lens was avoided, although slight insults to the lens did not result in cataract formation in our hands. Incidence of cataract formation was reduced further by modifications to the insertion method of the 33 gauge blunt needle. As the needle is aimed nasally and advanced through the anterior chamber toward the posterior pole, care was taken to avoid trauma to lens and iris while guiding the needle through the zonules and between lens and iris, thereby reducing cataract formation and acute miosis respectively. On occasion, upon entry into the subretinal matrix, a retinal vessel was damaged resulting in hemorrhage into the vitreous. These complications were difficult to foresee and no differences in ERG b-wave amplitudes or retinal histology were

noted in these cases. In our experience, incisional corneal trauma or puncture wound healing did not result in appreciable corneal opacification

Subretinal delivery could be assessed with a binocular indirect ophthalmoscope. This method, however, required some familiarity with operating an indirect ophthalmoscope and the interpretation of fundus changes. Alternatively, and more conveniently, we found that addition of fluorescein to the injection mixture allowed visualization of the injection as it proceeded and helped to locate and assess the retinal bleb under the dissecting microscope. In addition, the use of fluorescein simplified photography of the injection bleb (Figure 2) and reflux of the injection mixture could readily be observed. A successful subretinal delivery was established when the retinal vessels were seen to extend over the surface of the green bleb (Figure 2). Injections into the vitreous resulted in the green dye obscuring the retinal vessels. Subchoroidal injections in albino animals did not produce a green bleb, instead a faint, flattened and diffuse area of green color would be observed. In pigmented animals, the green color of fluorescein would be masked and made imperceptible by the pigment in RPE and choroid. The fluorescein administered with the injection was cleared rapidly and completely from the rodent eye. The following day, fluorescein was not detectable with either fluorescence indirect ophthalmoscopy or fluorescence fundus pho-

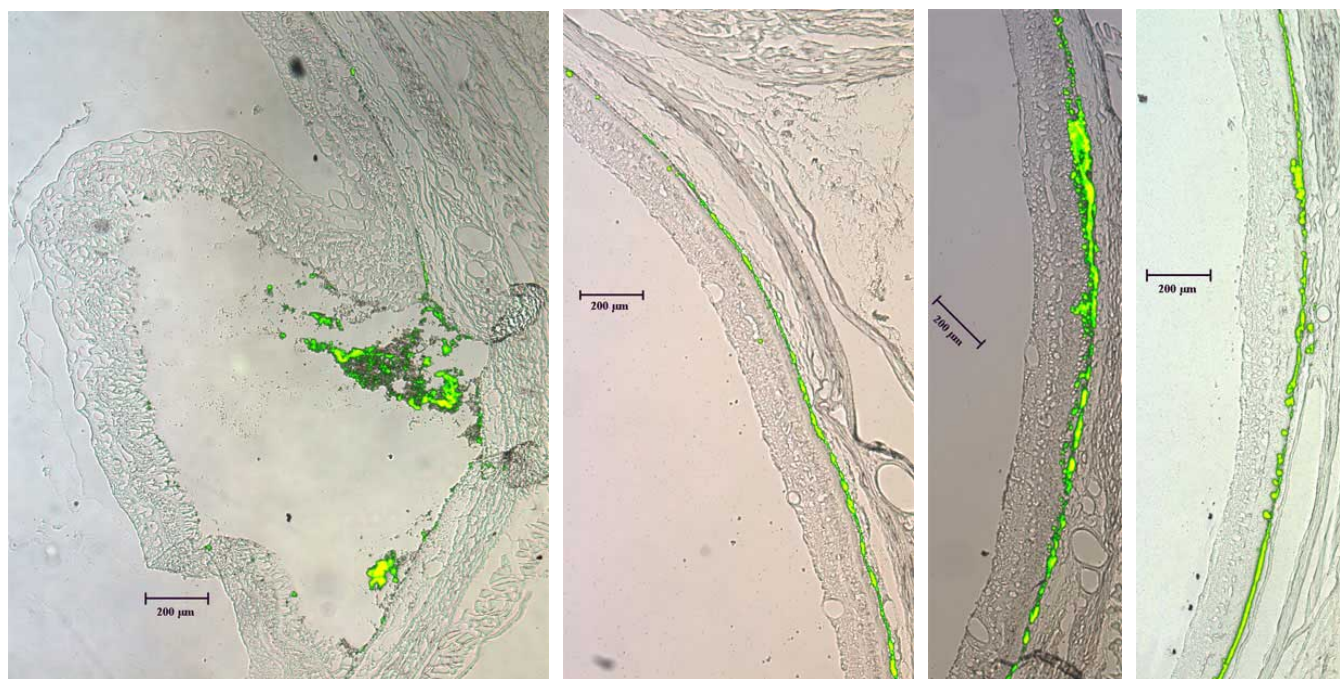


Figure 3. Sections of rat eyes after injection with fluorescent microspheres. Rat eyes were injected with 2 μ l of fluorescent microspheres followed by sampling of rats 2 h post-injection (A), 1 day post-injection (B), 3 days post-injection (C), and 7 days post-injection (D). The rats were sacrificed by carbon dioxide asphyxiation followed by cardiac perfusion with 4% paraformaldehyde. Cryostat sections of 15 μ m were prepared and viewed under fluorescence and bright field microscopy. A massive retinal detachment was visible immediately following the subretinal injection of the fluorescent microsphere suspension (A). A cluster of beads remained visible after fixation and sectioning, although most of the injected beads were lost during the processing of the sections. The retina was completely re-attached one day after the injection (B). The fluorescent microspheres spread over an area that comprised approximately 50% to 60% of the total retinal area (B). In subsequent days (C and D), the retinal area with fluorescent beads remained constant.

tography (data not shown). The presence of fluorescein in the injection mixtures did not interfere with electrophysiological or histological analyses of the injected rat eye.

A trans-scleral approach to subretinal injections requires surgical preparation of conjunctiva for access to the posterior sclera. These results in potential complications including bleeding, increased chances of infection and need for suturing. Compared to a trans-scleral approach, the advantages of the method described here were the ease of learning the procedure, the simplicity of injecting large numbers of eyes, the lack of surgical preparations and the high success rate.

Retinal reattachment after fluorescent microsphere injection: Rat eyes (n=16) were injected subretinally with 2 μ l suspension of microspheres in PBS. Eyes were fixed by cardiac perfusion either immediately (within 2 h) following the injection, one day post-injection, 3 days post-injection or 1 week post-injection. Each whole eye was sectioned and size

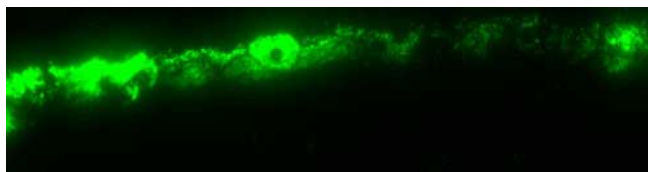


Figure 4. Phagocytotic activity of RPE cells after injection of fluorescent microspheres. Rats were injected with 2 μ l of 1 μ m fluorescent microspheres and processed as described in Figure 3. Only the fluorescent image is shown. The hexagonal outline typical of RPE cells is visible due to the fluorescent spheres within the cell. In some RPE cells, the nucleus can be seen as the dark spot within the cell. The RPE cells retained their ability for phagocytosis after subretinal injection and consequent retinal detachment.

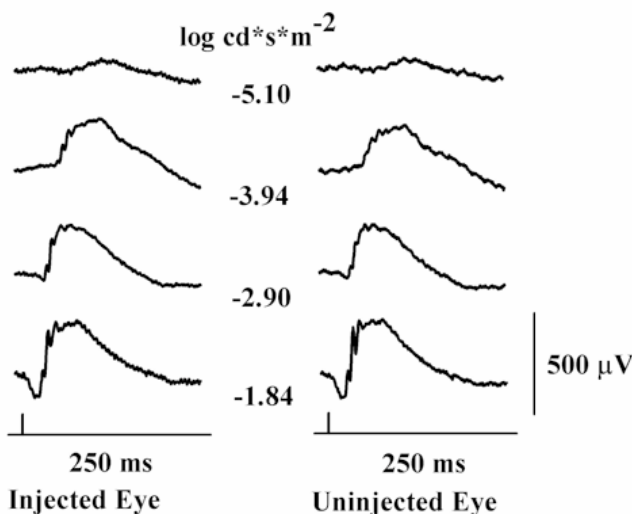


Figure 5. ERG traces of subretinally injected eye and uninjected eye. Rat eyes were injected subretinally with 2 μ l of PBS fluorescein mixture or not injected. After dark-adaptation overnight, ERG traces were recorded on a UTAS-E 2000 Visual Electrodiagnostic System one week after subretinal injections. Flash intensities of blue light varied from -5.1 to -1.84 cd*s*m^{-2} . Each trace is the average of five recordings.

and spread of the subretinal bleb was assessed. Bright field and fluorescent images of representative 15 μ m unstained cryostat sections were merged (Figure 3). Immediately after the injection, a large retinal bleb was clearly visible with fluorescent beads in approximately 20% (n=4) of the total retinal surface (Figure 3A). The following day the fluorescent beads had spread over approximately 50% to 60% (n=4) of the retinal area with the retina completely reattached to the retinal pigment epithelial cell layer (Figure 3B). At the third day (n=4; Figure 3C) and one-week post injection (n=4; Figure 3D), the size of the area with fluorescent spheres remained the same,

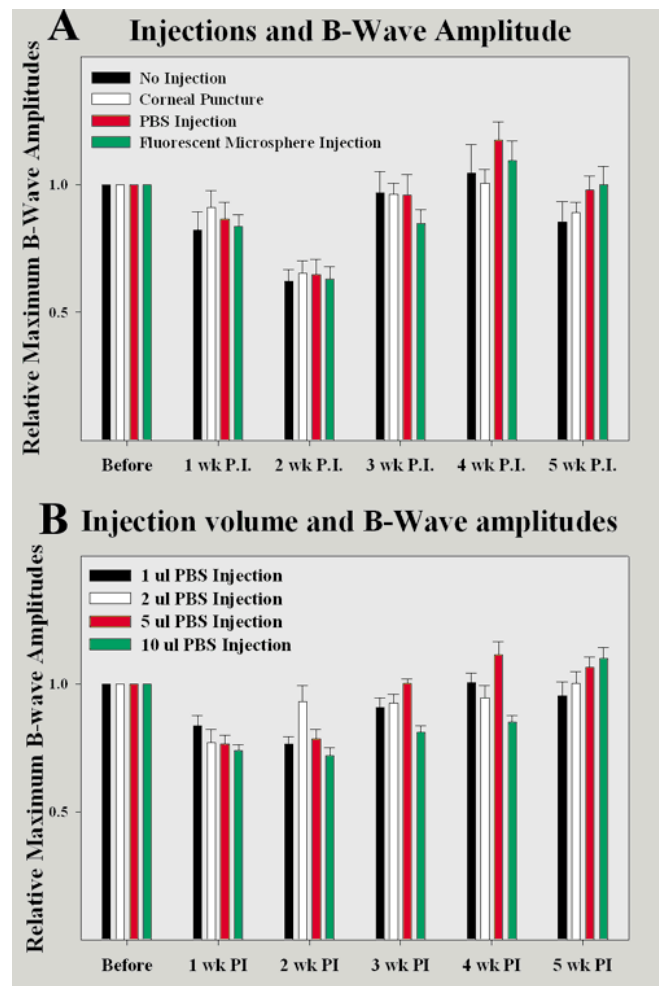


Figure 6. Average relative b-wave amplitudes after subretinal injections of rat eyes. Scotopic full field ERG measurements were done in dark-adapted rats that were flashed with increasing intensities of blue light (-5.1 to -1.84 cd*s*m^{-2}). Measurements were taken pre-injection and weekly for 5 weeks post injection. The b-wave average of all eyes within a group was plotted with standard error bars; PI stands for post-injection. **A:** Average relative b-wave amplitudes after subretinal injections into rat eyes. No significant differences were detected between either group over a period of 5 weeks. **B:** Average relative b-wave amplitudes after subretinal injection of an increasing volume of PBS-fluorescein mixture in rat eyes. No significant differences were detected between 1, 2, 5, or 10 μ l. It appeared that the eyes injected with 10 μ l trailed in recovery.

with most of the beads phagocytized by the retinal pigment epithelium cells (Figure 4). In our hands, the retinal histology of eyes injected subretinally was indistinguishable from retinas in non-injected eyes (data not shown). We concluded that histological integrity of retina and RPE cells is not affected by the subretinal injection procedure. Furthermore, the RPE cells remain functional as they are capable of phagocytosis of the injected microspheres (Figure 4).

Electroretinographic analysis of injected eyes: The effect of the subretinal injections on retinal function was assessed by ERG analysis simultaneously on both eyes of overnight dark-adapted rats with increasing intensities of blue light. ERG b-wave amplitudes were measured before the subretinal injection procedure. The eyes were divided into four groups: no injection (n=4), puncture of the cornea (n=5), injection with 2 μ l (n=5) of PBS-fluorescein mixture, and injection with 2 μ l of 1 μ m fluorescent spheres (n=4). An example of ERG traces recorded from an injected and non-injected eye are shown in Figure 5. The average and standard error of the relative ERG b-wave amplitudes for each injection protocol are plotted in Figure 6A. From these data, we concluded that the injection procedures did not impact the ERG b-wave amplitude. No significant differences existed between non-injected eyes, eyes with punctured corneas, PBS-fluorescein mixture injected eyes or fluorescent microsphere injected eyes. A 35% reduction in amplitude is observed at two weeks post-injection. This decrease in ERG amplitude was highly reproducible since we consistently observed this in more than 50 rat eyes. The loss in amplitude and subsequent recovery was similar for either injection protocol (Figure 6A).

We hypothesized that this reduction of ERG b-wave amplitude could be caused by the intense light source required during the injection procedure under the dissecting microscope [31]. The fully dilated non-injected eyes were the contralateral eyes of the microsphere-injected eyes and thereby exposed to the intense light source. The decrease in ERG amplitude in the non-injected eyes was therefore consistent with our hypothesis. The hypothesis predicts that if rat eyes were shielded from the intense light source, the ERG b-wave amplitude should remain at pre-injection levels over the five-week period. However, we found a similar decrease in ERG b-wave amplitude after two weeks in eyes (n=2) not exposed to the intense light source (data not shown). Therefore, our hypothesis was rejected. Consequently, we concluded that the decrease in ERG b-wave amplitude after two weeks did not result from the injection procedure.

To determine the effect of injection volume on retinal function, rat eyes were divided into four groups, each receiving subretinally increasing volumes of PBS-fluorescein mixture. Eyes in each group were injected with either 1 μ l (n=6), 2 μ l (n=6), 5 μ l (n=6) or 10 μ l (n=6) of PBS-fluorescein mixture. As described above, baseline ERG measurements were done prior to the injections and followed by weekly ERG measurements over a period of five weeks (Figure 6B). No significant difference could be observed between either injection group, although a slight trailing in recovery of b-wave amplitudes could be observed in the eyes injected with 10 μ l of PBS-

fluorescein mixture. We concluded from these findings that rat eyes could be injected subretinally with at least 10 μ l without loss of functional integrity.

We extrapolated based on the approximately five fold difference in retinal area between the rat and mouse, the maximum volume for subretinal injection in the smaller mouse eye should not exceed one to 2 μ l. Our experience with mice parallels our experience with rats, albeit that success rates were slightly lower (80%), and incidence of cataract slightly higher (10%) in mice. We attributed this difference to the much smaller eyes in mice.

ACKNOWLEDGEMENTS

The authors wish to thank Doug Yasumura (UCSF School of Medicine, Beckman Vision Center, San Francisco, USA) for the helpful discussions on his approach to subretinal injections. We wish to thank Dr. Adriana Di Polo (University of Montreal, Montreal, Canada) for her help and suggestions with regard to cardiac perfusion. Finally, the authors wish to thank The Foundation Fighting Blindness for their support for this work (T-GT-0499-0027).

REFERENCES

- Hauswirth WW, Lewin AS, Zolotukhin S, Muzyczka N. Production and purification of recombinant adeno-associated virus. *Methods Enzymol* 2000; 316:743-61.
- Guy J, Qi X, Muzyczka N, Hauswirth WW. Reporter expression persists 1 year after adeno-associated virus-mediated gene transfer to the optic nerve. *Arch Ophthalmol* 1999; 117:929-37.
- Guy J, Qi X, Hauswirth WW. Adeno-associated viral-mediated catalase expression suppresses optic neuritis in experimental allergic encephalomyelitis. *Proc Natl Acad Sci U S A* 1998; 95:13847-52.
- Lewin AS, Drenser KA, Hauswirth WW, Nishikawa S, Yasumura D, Flannery JG, LaVail MM. Ribozyme rescue of photoreceptor cells in a transgenic rat model of autosomal dominant retinitis pigmentosa. *Nat Med* 1998; 4:967-71.
- Flannery JG, Zolotukhin S, Vaquero MI, LaVail MM, Muzyczka N, Hauswirth WW. Efficient photoreceptor-targeted gene expression in vivo by recombinant adeno-associated virus. *Proc Natl Acad Sci U S A* 1997; 94:6916-21.
- Zolotukhin S, Potter M, Hauswirth WW, Guy J, Muzyczka N. A "humanized" green fluorescent protein cDNA adapted for high-level expression in mammalian cells. *J Virol* 1996; 70:4646-54.
- Bennett J, Maguire AM. Gene therapy for ocular disease. *Mol Ther* 2000; 1:501-5.
- Bennett J, Anand V, Acland GM, Maguire AM. Cross-species comparison of in vivo reporter gene expression after recombinant adeno-associated virus-mediated retinal transduction. *Methods Enzymol* 2000; 316:777-89.
- Anand V, Chirmule N, Fersh M, Maguire AM, Bennett J. Additional transduction events after subretinal readministration of recombinant adeno-associated virus. *Hum Gene Ther* 2000; 11:449-57.
- Bennett J, Maguire AM, Cideciyan AV, Schnell M, Glover E, Anand V, Aleman TS, Chirmule N, Gupta AR, Huang Y, Gao GP, Nyberg WC, Tazelaar J, Hughes J, Wilson JM, Jacobson SG. Stable transgene expression in rod photoreceptors after recombinant adeno-associated virus-mediated gene transfer to monkey retina. *Proc Natl Acad Sci U S A* 1999; 96:9920-5.

11. Bennett J, Duan D, Engelhardt JF, Maguire AM. Real-time, noninvasive in vivo assessment of adeno-associated virus-mediated retinal transduction. *Invest Ophthalmol Vis Sci* 1997; 38:2857-63.
12. Ali RR, Sarra GM, Stephens C, Alwis MD, Bainbridge JW, Munro PM, Fauser S, Reichel MB, Kinnon C, Hunt DM, Bhattacharya SS, Thrasher AJ. Restoration of photoreceptor ultrastructure and function in retinal degeneration slow mice by gene therapy. *Nat Genet* 2000; 25:306-10.
13. Ali RR, Reichel MB, De Alwis M, Kanuga N, Kinnon C, Levinsky RJ, Hunt DM, Bhattacharya SS, Thrasher AJ. Adeno-associated virus gene transfer to mouse retina. *Hum Gene Ther* 1998; 9:81-6.
14. Reichel MB, Ali RR, Hunt DM, Bhattacharya SS. Gene therapy for retinal degeneration. *Ophthalmic Res* 1997; 29:261-8.
15. Ali RR, Reichel MB, Thrasher AJ, Levinsky RJ, Kinnon C, Kanuga N, Hunt DM, Bhattacharya SS. Gene transfer into the mouse retina mediated by an adeno-associated viral vector. *Hum Mol Genet* 1996; 5:591-4.
16. Takahashi M, Miyoshi K, Verma IM, Gage FH. Rescue from photoreceptor degeneration in the rd mouse by human immunodeficiency virus vector-mediated gene transfer. *J Virol* 1999; 73:7812-6.
17. Miyoshi H, Takahashi M, Gage FH, Verma IM. Stable and efficient gene transfer into the retina using an HIV-based lentiviral vector. *Proc Natl Acad Sci U S A* 1997; 94:10319-23.
18. Cayouette M, Behn D, Sendtner M, Lachapelle P, Gravel C. Intraocular gene transfer of ciliary neurotrophic factor prevents death and increases responsiveness of rod photoreceptors in the retinal degeneration slow mouse. *J Neurosci* 1998; 18:9282-93.
19. Cayouette M, Gravel C. Adenovirus-mediated gene transfer of ciliary neurotrophic factor can prevent photoreceptor degeneration in the retinal degeneration (rd) mouse. *Hum Gene Ther* 1997; 8:423-30.
20. Rakoczy PE, Shen WY, Lai M, Rolling F, Constable IJ. Development of gene therapy-based strategies for the treatment of eye diseases. *Drug Development Research* 1999; 46:277-85.
21. Rolling F, Shen WY, Tabarias H, Constable I, Kanagasalingam Y, Barry CJ, Rakoczy PE. Evaluation of adeno-associated virus-mediated gene transfer into the rat retina by clinical fluorescence photography. *Hum Gene Ther* 1999; 10:641-8.
22. Rakoczy PE, Lai MC, Baines MG, Spilsbury K, Constable IJ. Expression of cathepsin S antisense transcripts by adenovirus in retinal pigment epithelial cells. *Invest Ophthalmol Vis Sci* 1998; 39:2095-104.
23. da Cruz L, Rakoczy PE, Constable IJ. Expression of transgenes in human and rat retinal pigment epithelium in vitro using an adenoviral vector. *Aust N Z J Ophthalmol* 1996; 24:78-81.
24. da Cruz L, Rakoczy P, Perricaudet M, Constable IJ. Dynamics of gene transfer to retinal pigment epithelium. *Invest Ophthalmol Vis Sci* 1996; 37:2447-54.
25. Price J, Turner D, Cepko C. Lineage analysis in the vertebrate nervous system by retrovirus-mediated gene transfer. *Proc Natl Acad Sci U S A* 1987; 84:156-60.
26. Turner DL, Cepko CL. A common progenitor for neurons and glia persists in rat retina late in development. *Nature* 1987; 328:131-6.
27. Faktorovich EG, Steinberg RH, Yasumura D, Matthes MT, LaVail MM. Photoreceptor degeneration in inherited retinal dystrophy delayed by basic fibroblast growth factor. *Nature* 1990; 347:83-6.
28. Silverman MS, Hughes SE. Photoreceptor rescue in the RCS rat without pigment epithelium transplantation. *Curr Eye Res* 1990; 9:183-91.
29. Hawes NL, Smith RS, Chang B, Davisson M, Heckenlively JR, John SW. Mouse fundus photography and angiography: a catalogue of normal and mutant phenotypes. *Mol Vis* 1999; 5:22 .
30. Bayer AU, Mittag T, Cook P, Brodie SE, Podos SM, Maag KP. Comparisons of the amplitude size and the reproducibility of three different electrodes to record the corneal flash electroretinogram in rodents. *Doc Ophthalmol* 1999; 98:233-46.
31. Kirkness CM. Do ophthalmic instruments pose a hazard of light-induced damage to the eye? In: Cronly-Dillon J, Rosen ES, Marshall J, editors. *Hazards of light: myths and reality*. Eye and skin. Proceedings of the First International Symposium of the Northern Eye Institute; 1985 July; Manchester, England. Oxford: Pergamon Press; 1986. p. 179-86.